AGU PUBLICATIONS

JGR

Journal of Geophysical Research: Biogeosciences

RESEARCH ARTICLE
10.1002/2015JG003266

Key Points:
- BrGDGT distributions are consistent among catchment, river, and estuarine environments
- In situ aquatic brGDGT production has limited impact on the applicability of the MBT′/CBT paleothermometer in Simpson Lagoon, AK
- MBT′-/CBT-derived temperatures are consistent with instrumental summer air temperature

Supporting Information:
- Supporting Information S1

Correspondence to:
A. J. M. Hanna,
annie.m@utexas.edu

Citation:
Hanna, A. J. M., T. M. Shanahan, and M. A. Allison (2016), Distribution of branched GDGTs in surface sediments from the Colville River, Alaska: Implications for the MBT′/CBT paleothermometer in Arctic marine sediments, *J. Geophys. Res. Biogeosci.*, *121*, 1762–1780, doi:10.1002/2015JG003266.

Received 31 OCT 2015
Accepted 20 JUN 2016
Accepted article online 23 JUN 2016
Published online 5 JUL 2016

©2016. American Geophysical Union.
All Rights Reserved.

Distribution of branched GDGTs in surface sediments from the Colville River, Alaska: Implications for the MBT′/CBT paleothermometer in Arctic marine sediments

Andrea J. M. Hanna[1], Timothy M. Shanahan[2], and Mead A. Allison[3,4]

[1]Institute for Geophysics, Jackson School of Geosciences, University of Texas at Austin, Austin, Texas, USA, [2]Department of Geosciences, Jackson School of Geosciences, University of Texas at Austin, Austin, Texas, USA, [3]Department of Earth and Environmental Sciences, Tulane University, New Orleans, Louisiana, USA, [4]The Water Institute of the Gulf, Baton Rouge, Louisiana, USA

Abstract Significant climate fluctuations in the Arctic over the recent past, and additional predicted future temperature changes, highlight the need for high-resolution Arctic paleoclimate records. Arctic coastal environments supplied with terrigenous sediment from Arctic rivers have the potential to provide annual to subdecadal resolution records of climate variability over the last few millennia. A potential tool for paleotemperature reconstructions in these marine sediments is the revised methylation index of branched tetraethers (MBT′)/cyclization ratio of branched tetraethers (CBT) proxy based on branched glycerol dialkyl glycerol tetraethers (brGDGTs). In this study, we examine the source of brGDGTs in the Colville River, Alaska, and the adjacent Simpson Lagoon and reconstruct temperatures from Simpson Lagoon sediments to evaluate the applicability of this proxy in Arctic estuarine environments. The Colville catchment soils, fluvial sediments, and estuarine sediments contain statistically similar brGDGT distributions, indicating that the brGDGTs throughout the system are soil derived with little alteration from in situ brGDGT production in the river or coastal waters. Temperatures reconstructed from the MBT′/CBT indices for surface samples show good agreement with regional summer (June through September) temperatures, suggesting a seasonal bias in Arctic temperature reconstructions from the Colville system. In addition, we reconstruct paleotemperatures from an estuarine sediment core that spans the last 75 years, revealing an overall warming trend in the twentieth century that is consistent with trends observed in regional instrumental records. These results support the application of this brGDGT-based paleotemperature proxy for subdecadal-scale summer temperature reconstructions in Arctic estuaries containing organic material derived from sediment-laden, episodic rivers.

1. Introduction

The Arctic has experienced significant climate variability over the last few centuries and is anticipated to be one of the regions most sensitive to future climate changes [e.g., *Overpeck et al.*, 1997; *Holland and Bitz*, 2003; *Serreze and Barry*, 2011; *Intergovernmental Panel on Climate Change*, 2013; *Schuur et al.*, 2015]. In the last century alone, the Alaskan Arctic has undergone increases in average air and permafrost temperature [*Serreze et al.*, 2000; *Hinzman et al.*, 2005; *Jorgenson et al.*, 2006], increasingly rapid shoreline retreat [*Mars and Houseknecht*, 2007; *Jones et al.*, 2009], and increases in the melting rates of mountain glaciers [*Evison et al.*, 1996], while the extent of snow cover and sea ice has decreased [*Stone et al.*, 2001; *Mahoney et al.*, 2007]. An understanding of past climate changes in the Arctic is needed to place these recent changes in the context of longer-term natural climate variability and to help constrain future climate projections.

One challenge is that quantitative and high-resolution (annual to subdecadal) records of temperature variability from the Arctic (e.g., tree rings and lake sediments) are relatively sparse and instrumental records are typically short (<60 years) or discontinuous [*Bradley*, 1990; *Besonen et al.*, 2008]. This lack of data significantly limits our understanding of past circum-Arctic temperature variations and our ability to understand the large-scale controls on these changes [*McKay and Kaufman*, 2014]. In order to better understand the temporal and spatial patterns of past temperature variations and their magnitudes, new archives and quantitative paleotemperature proxies are critically needed. An underutilized archive of past climate change in the Arctic is deltaic marine sediments [*Bianchi and Allison*, 2009]. These systems can provide

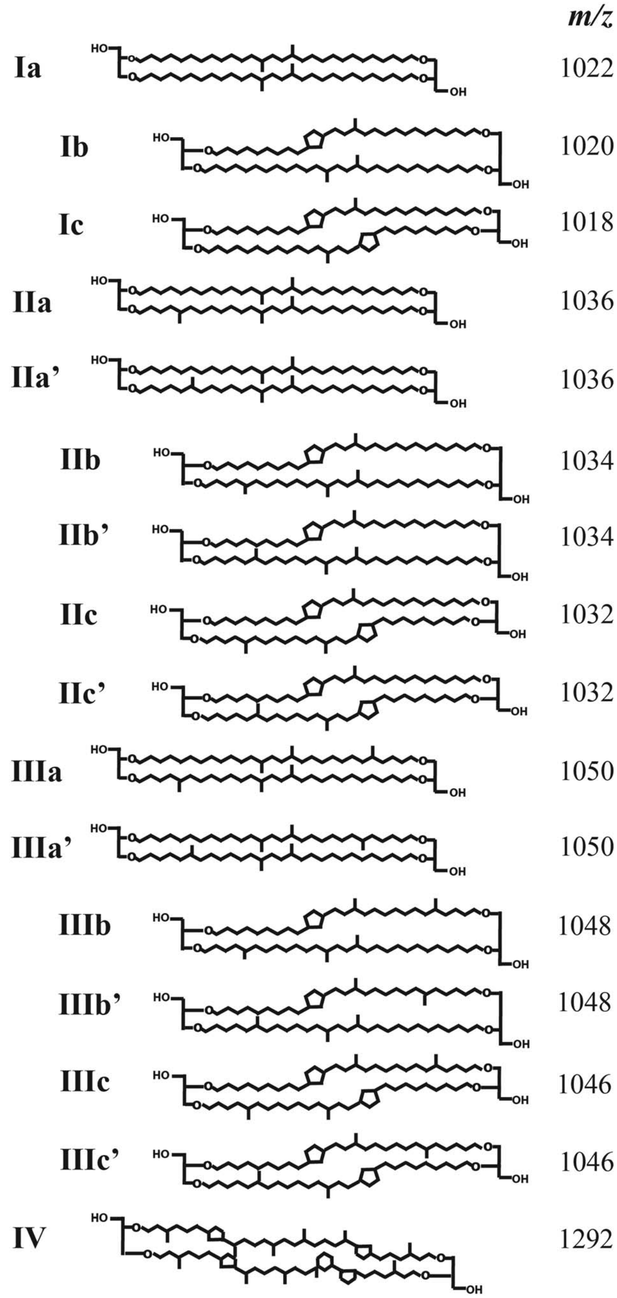

Figure 1. Structures of branched GDGTs, including the recently identified 6-methyl brGDGT isomers and crenarchaeol (IV).

continuous, undisturbed, and high-resolution archives of changes in the marine and terrestrial environment. One potential proxy for generating past temperature reconstructions from coastal marine sediments is the methylation index of branched tetraethers/cyclization ratio of branched tetraethers (MBT/CBT) index [*Weijers et al*., 2007a; *Rueda et al*., 2009; *Bendle et al*., 2010]. The MBT and CBT indices are based on the relative abundances of branched glycerol dialkyl glycerol tetraethers (brGDGTs) preserved in the sediment record. BrGDGTs are microbial membrane lipids found primarily in soil organic material stored in globally distributed peats [*Weijers et al*., 2006], soils [*Weijers et al*., 2007b; *Peterse et al*., 2012], lake sediments [*Blaga et al*., 2009; *Tierney et al*., 2010; *Loomis et al*., 2011; *Pearson et al*., 2011], and marine sediments [*Weijers et al*., 2007a; *Rueda et al*., 2009; *Bendle et al*., 2010; *De Jonge et al*., 2015, 2016]. The nine individual brGDGTs utilized in the MBT/CBT index contain varying numbers of methyl substituents (4–6) and cyclopentyl moieties (0–2) on linear C_{28} alkyl chains (Figure 1). Previous studies have shown that the relative distributions of these brGDGTs are controlled primarily by temperature and soil pH [*Weijers et al*., 2007b], and empirical relationships between the degree of methylation and cyclization (MBT and CBT indices) and continental mean air temperature have been developed using globally distributed soils (i.e., the soil MBT/CBT paleothermometer [*Weijers et al*., 2007b; *Peterse et al*., 2012; *Anderson et al*., 2014; *Ding et al*., 2015]). In addition to the nine brGDGTs originally described by *Sinninghe Damsté et al*. [2000] and *Weijers et al*. [2006], a novel set of six brGDGT isomers containing methyl groups at the 6 position have recently been identified by *De Jonge et al*. [2013, 2014a] (Figure 1). These globally abundant 6-methyl compounds have been shown to coelute with the 5-methyl brGDGTs utilized in the MBT/CBT paleothermometer and exhibit a strong relationship with soil pH [*De Jonge et al*., 2013, 2014a].

BrGDGTs were originally thought to have an entirely terrigenous origin, with the dominant source of brGDGTs in marine sediments derived from catchment soils transported to the coastal ocean via rivers [*Hopmans et al*., 2004]. Recent observations indicate that significant in situ aquatic production of brGDGTs, within both freshwater and marine environments, may occur as well. This may complicate the use of these molecular biomarkers as temperature proxies in environments containing mixed aquatic and terrigenously sourced organic matter, since the temperature effect on brGDGT distributions differs significantly between terrestrial and aquatic systems [*Peterse et al.*, 2009; *Sinninghe Damsté et al.*, 2009; *Tierney et al.*, 2010; *Loomis et al.*, 2011; *Zhu et al.*, 2011; *Zell et al.*, 2013b, 2014; *De Jonge et al.*, 2014b, 2015]. Previous studies of brGDGT distributions in modern rivers have hypothesized that in situ production within the riverine water column may be seasonally variable, with decreased aquatic production during high water periods [*Zell et al.*, 2013a; *De Jonge et al.*, 2015]. If this is the case, the relative contribution of terrigenous and aquatic brGDGTs being delivered to coastal marine sediments will depend strongly on river hydrology. Most small to moderate sized Arctic river systems are extremely flood prone, commonly carrying 40–80% of their annual volume of water during the spring freshet [*Gordeev et al.*, 1996; *Rember and Trefry*, 2004]. In such systems aquatic brGDGT production is likely to be minimized, leading to a signal that is dominated by terrigenous brGDGT contributions. However, the use of the MBT/CBT paleothermometer in fluvial and marine sediments may also be complicated by the influx of sediment eroded from aged sediment deposits containing brGDGT distributions characteristic of the temperature/pH conditions at the time of soil formation [*De Jonge et al.*, 2015; *Dogrul Selver et al.*, 2015; *Sparkes et al.*, 2015]. The contribution of these aged-brGDGTs to nearshore marine sediments may be particularly significant in the Arctic, as the rates of shoreline retreat/coastal erosion are among the highest in the world [*Rachold et al.*, 2000; *Jones et al.*, 2009].

To examine the processes controlling brGDGT production and delivery in ephemeral Arctic river systems, and their fidelity for paleotemperature reconstructions on decadal to centennial timescales, we analyzed the distribution of brGDGTs in river, catchment soils, and estuarine sediments distributed along the Colville River catchment and the adjacent Simpson Lagoon, Alaska (approximately 70.5°N, 150°W; Figure 2). Previous studies of brGDGTs in rivers have focused mostly on large river systems (e.g., Yangtze, Amazon, and Yenisei [*Zhu et al.*, 2011; *Zell et al.*, 2013a, 2013b; *De Jonge et al.*, 2014b]), and much less is known about the sources of brGDGTs in smaller, flood-prone systems like the Colville, which are much more common in the Arctic. We complement the analysis of modern surface sediments in the Colville catchment with a high-resolution record of downcore variations in brGDGT-derived temperatures from Simpson Lagoon sediments spanning the last 75 years and compare this record against regional instrumental temperature records to evaluate the accuracy of brGDGT-derived temperature reconstructions on subdecadal timescales. This study provides new insight for the use of MBT/CBT paleothermometry in Arctic estuaries and potentially in other nearshore sediment repositories off sediment-laden, episodic rivers.

2. Regional Setting

The Colville River, located on Alaska's North Slope, is a ~600 km long braided river originating in the Northern Brooks Range (elevations >3000 m). It flows northward across the Arctic foothills and Arctic coastal plain before emptying into the Beaufort Sea (Figure 2a). With an area of 53,000 km^2, the Colville catchment is the largest on Alaska's North Slope [*Walker*, 1998; *Walker and Hudson*, 2003]. The Arctic foothills and coastal plain are primarily underlain by Triassic to Quaternary siliciclastic deposits, with Cretaceous and Pliocene/Pleistocene formations outcropping along the western side of the river catchment throughout the lower reaches of the river [*Moore et al.*, 1994; *Flaig et al.*, 2011]. The watershed contains organic-rich soils with a silt and sand-sized mineral component [*Jorgenson and Brown*, 2005]. One of the more unique features of the Colville catchment is that it is among the largest rivers in the Arctic located entirely within the zone of continuous permafrost (larger systems such as the Mackenzie extend southward into the sub-Arctic). The permafrost soils in the Arctic foothills and coastal plain range in thickness between 250 and >600 m, with an active layer extending 20 cm to >1 m below the surface [*Lachenbruch and Marshall*, 1969; *Osterkamp and Payne*, 1981; *Eisner et al.*, 2005].

The low mean annual air temperature on the North Slope (e.g., -11°C at Umiat, AK, and Barrow, AK, averaged from 1990 to 2000; NOAA National Climate Data Center) results in 7–9 months of snow and ice cover per year, with snow beginning to accumulate in late September/early October [*Walker and Hudson*, 2003]. During this time, water discharge from the Colville River essentially ceases due to the presence of thick channel ice (>2 m [*Walker and Hudson*, 2003]). The breakup of the river ice and snow melt in the catchment occurs during late May to early June, resulting in a late spring/early summer flood. The Colville River is particularly flood prone; 62% of the annual sediment load (6×10^6 t yr^{-1}) is transported during only 4% of the year, with water

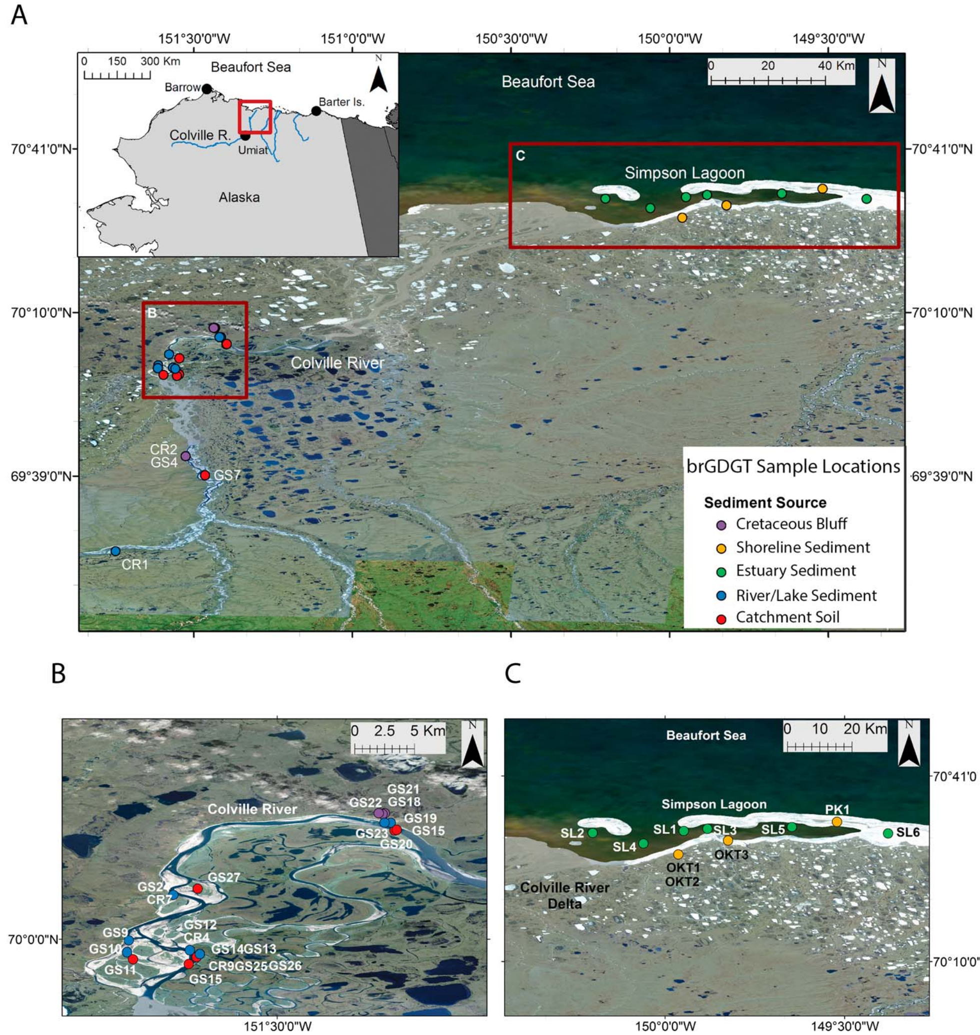

Figure 2. (a) Map of the Colville River/Simpson Lagoon study area with locations of soil and sediment samples collected during the August 2010 and August 2012 field studies. Samples are categorized by source, differentiating samples collected from the catchment, river, estuary, shoreline, and Cretaceous bluffs. Detailed views of the (a) northern Colville River study site and the (b) Simpson Lagoon site are shown. Landsat images are from the Alaska Statewide Digital Mapping Initiative and the UAF Geographic Information Network of Alaska (http://www.alaskamapped.org).

discharge reaching 6000 $m^3\ s^{-1}$ and suspended solids concentrations as great as 600 mg L^{-1} [*Arnborg et al.*, 1967; *Walker and Hudson*, 2003; *Rember and Trefry*, 2004]. During the freshet, the numerous floodplain lakes and sloughs along the Colville are flooded with water from the river's main stem [*Craig and McCart*, 1975; *Walker*, 1975].

Simpson Lagoon, a partially enclosed back-barrier estuary, is located adjacent to the Colville River Delta on the inner shelf of the Beaufort Sea (Figures 2a and 2c). The lagoon extends 35 km in length and 3–6 km in width and is bordered to the north by the Jones Barrier Islands. The shallow depths (commonly < 2.5 m) result in landfast ice formation throughout the majority of the lagoon for a duration of 8–9 months per year [*Reimnitz et al.*, 1978]. The interbedded, estuarine sediments in Simpson Lagoon [*Hanna et al.*, 2014] display minimal evidence of physical disturbance from ice processes (i.e., ice gouging), a common occurrence in Arctic shelf environments. This was attributed by these authors, in part, to the protection provided by the formation of landfast ice and the presence of the Jones Barrier Islands. In addition, sediments within the lagoon exhibit relatively high rates of sediment accumulation (0.07–0.46 cm yr^{-1}), with the majority of sediment and organic material sourced from the Colville River in western lagoon areas proximal to the delta, and an increasing sediment contribution from shoreline erosion in eastern Simpson Lagoon [*Schreiner et al*., 2013; *Hanna et al*., 2014].

3. Materials and Methods

3.1. Field Study and Sampling

Samples from the Colville catchment and adjacent Simpson Lagoon were collected during two separate field studies. In August 2010, six marine sediment cores (SL1–SL6, Figure 2c) were collected in Simpson Lagoon using a Rossfelder P-3 submersible vibracorer at sites displaying thick estuarine sediment fill (see *Hanna et al*. [2014] for more detail). In addition, grab samples were collected from tundra soil on Pingok Island ($n = 1$), and from the shoreline bluffs near Oliktok Point ($n = 3$) (Figure 2c). The second field study was conducted in August 2012 along the Colville River, extending from 70 to 170 km upstream of the Colville Delta (Figure 2b). Twenty surface grab samples (upper ~5–10 cm of soil/sediment) were collected from a variety of sedimentary environments along the river and include catchment soil ($n = 7$), sediment from river sloughs and floodplain lakes ($n = 11$), and poorly lithified Pliocene/Pleistocene (Gubik Formation, $n = 2$), and Cretaceous (Prince Creek Formation, $n = 5$) outcrops along the west bank of the Colville River channel (Figures 2a and 2b). In addition, five, ~50 cm push cores were collected along the river in sloughs and floodplain lakes. The location and depositional environment of each sample is presented in the supporting information (Table S1). Simpson Lagoon cores were subsampled at 1 cm intervals, while cores collected in the Colville catchment were sampled using a 2 cm sampling scheme.

Samples from the floodplain lakes are grouped with fluvial sediment samples in this study, under the assumption that sediment is primarily entering the floodplain lakes during the freshet and subsequent summer floods when these lakes connect to the river's main stem. Floodplain lakes that connect with rivers during high flow periods have been shown to display similar brGDGT distributions to riverine material in previous studies [*Zell et al*., 2013b; *Peterse et al*., 2014]. Although suspended particulate matter (SPM) was not collected from the Colville River or the floodplain lakes, previous studies have shown riverbed sediment brGDGT distributions to correlate well with that of SPM in other river systems [*Zhang et al*., 2012; *Zell et al*., 2013b].

3.2. ^{137}Cs Geochronology

Modern (within the past ~60 years) sediment accumulation was identified in the Simpson Lagoon cores and two cores from floodplain lakes/sloughs using ^{137}Cs geochronology. Measurements of ^{137}Cs activities were obtained every 2 cm for the fine sediment fraction (<32 μm) by gamma spectrometry following the methods of *Hanna et al*. [2014]. ^{137}Cs, a radioisotope first produced in measureable quantities in fallout from the atmospheric testing of thermonuclear weapons, was present in all cores indicating modern sedimentation. The ^{137}Cs activity profile for Simpson Lagoon core SL2 is presented in *Hanna et al*. [2014] and is consistent with that of bomb-produced radionuclides, displaying a maximum activity peak corresponding to the 1963/1964 maximum global fallout from thermonuclear weapons testing. This depth horizon can be used as a chronostratigraphic marker to calculate an average sediment accumulation rate over this time interval. The accumulation rate in SL2 was calculated by dividing the depth of the ^{137}Cs activity peak by the elapsed time since the 1964 maximum global fallout. The age-depth model for SL2 was then created by extrapolation of the calculated sediment accumulation rate over the upper 35 cm of the core, requiring an assumption of constant sedimentation prior to the appearance of ^{137}Cs activity. Accumulation rate errors are a function of sample interval resolution and are calculated to be ± 0.04 cm yr^{-1}. However, additional uncertainty in the age-depth model may result from nonsteady state sediment accumulation, which is not captured by the ^{137}Cs methodology utilized in this study. All calendar ages determined by ^{137}Cs geochronology are reported in year CE (Common Era).

3.3. GDGT Analysis

3.3.1. Lipid Extraction

GDGT analyses were conducted on the Colville catchment grab samples, as well as the upper 1 cm of sediment from the Simpson Lagoon cores and the upper 2 cm of the floodplain lake cores. In addition, each 1 cm interval in the upper 35 cm of core SL2 from Simpson Lagoon was analyzed for brGDGTs (see Figure 2 for locations). The total lipid fraction was extracted following the methods of *Anderson et al*. [2014]. Lipids were extracted from approximately 5 g of sample with a solution of dichloromethane (DCM) and methanol

(MeOH, 9:1 vol/vol) using a microwave extraction system (MARS 5 Xpress, CEM Corporation). The extract was filtered through a Na_2SO_4 column fitted with a glass fiber filter to remove water and particulates. Samples were then dried using N_2 and dissolved in hexane. Elemental sulfur was removed by addition of activated copper powder followed by rinsing the samples with hexane (two times) and DCM (three times) through a glass fiber filter. Each filtered total lipid extract was fractionated into apolar, ketone, polar, and fatty acid fractions over an aminopropyl column using hexane, 4:1 hexane:DCM, 9:1 DCM:acetone, and 2% formic acid in DCM as eluents, respectively. The polar fractions to be used for GDGT analysis were subsequently blown down to dryness under nitrogen and redissolved in 1% isopropanol in hexane.

3.3.2. HPLC-MS

The polar fractions containing the branched and isoprenoid GDGTs were measured following the methods of *Schouten et al.* [2007] via high performance liquid chromatography-mass spectrometry (HPLC-MS). Analysis was conducted using an Agilent 1200 HPLC instrument fitted with a Prevail Cyano column coupled to a single quadrupole mass spectrometer. Separation was achieved by eluting the polar GDGTs with 1% isopropanol in hexane for 5 min followed by a linear increase to 1.5% isopropanol in hexane over a period of 28.1 min (modified from *Schouten et al.* [2007]). The flow rate was maintained at 0.2 ml min^{-1}. Detection of GDGTs was achieved in single ion monitoring mode using *m/z* 1292 for crenarchaeol and *m/z* 1022, 1020, 1018, 1036, 1034, 1032, 1050, 1048, and 1046 for the branched GDGTs Ia, Ib, Ic, IIa, IIb, IIc, IIIa, IIIb, and IIIc, respectively. The 6-methyl brGDGT isomers, identified by *De Jonge et al.* [2013, 2014a] (Figure 1), were not separately quantified with the utilized chromatography method as these isomers coeluted with the 5-methyl brGDGTs. Agilent Chemstation software was used to determine relative abundance by integrating the peak areas of the protonated molecule $[M + H]^+$. Blanks were run to identify any contamination during the lipid extraction and elution procedures.

3.3.3. Calculation of GDGT-Based Proxies

The branched and isoprenoid tetraether (BIT) index, indicating terrigenous versus marine origin, was calculated using the following equation modified from *Hopmans et al.* [2004]:

$$\text{BIT index} = (\text{Ia} + \text{IIa} + \text{IIa}' + \text{IIIa} + \text{IIIa}')/(\text{Ia} + \text{IIa} + \text{IIa}' + \text{IIIa} + \text{IIIa}' + \text{IV}) \quad (1)$$

Roman numerals Ia, IIa, IIa′, IIIa, and IIIa′ refer to the brGDGT structures illustrated in Figure 1, while IV is the isoprenoid GDGT, crenarchaeol. All equations presented here have been rewritten following *De Jonge et al.* [2014a] to illustrate that the 5- and 6-methyl brGDGTs were measured as coeluting compounds; however, further discussion will utilize the nomenclature from *Peterse et al.* [2012] in which the 6-methyl isomers are implicitly quantified with the 5-methyl brGDGTs.

The cyclization ratio of branched tetraethers (CBT) and degree of cyclization (DC) indices were calculated using equations from *Weijers et al.* [2007b] and *Sinninghe Damsté et al.* [2009], respectively. Here we employ the revised methylation index of branched tetraethers (MBT′) from *Peterse et al.* [2012].

$$\text{CBT} = -\log[(\text{Ib} + \text{IIb} + \text{IIb}')/(\text{Ia} + \text{IIa} + \text{IIa}')] \quad (2)$$

$$\text{DC} = (\text{Ib} + \text{IIb} + \text{IIb}')/(\text{Ia} + \text{Ib} + \text{IIa} + \text{IIa}' + \text{IIb} + \text{IIb}') \quad (3)$$

$$\text{MBT}' = (\text{Ia} + \text{Ib} + \text{Ic})/(\text{Ia} + \text{Ib} + \text{Ic} + \text{IIa} + \text{IIa}' + \text{IIb} + \text{IIb}' + \text{IIc} + \text{IIc}' + \text{IIIa} + \text{IIIa}') \quad (4)$$

The reconstructed pH and MAT (equations (5) and (6)) are functions of the CBT and MBT′ indices, and their equations are based on the global soil calibration of *Peterse et al.* [2012]. The residual standard mean error based on the *Peterse et al.* [2012] calibration is 0.8 for the pH calculation and 5.7°C for the MAT. MAT was also calculated using the original MBT index (equation (7)) from *Weijers et al.* [2007b], whose calibration has a residual standard mean error of 4.8°C. The calculated fractional abundances of brGDGTs, MBT/CBT values, pH, and MAT for each sample are presented in Tables S2–S5 in the supporting information.

$$\text{pH} = 7.9 - 1.97 \times \text{CBT} \quad (5)$$

$$\text{MAT} = 0.81 - 5.67 \times \text{CBT} + 31.0 \times \text{MBT}' \quad (6)$$

$$\text{MBT} = 0.122 + 0.187 \times \text{CBT} + 0.020 \times \text{MAT} \quad (7)$$

Errors in reconstructed temperatures were calculated using a bootstrapping method [*Efron*, 1979] following *Loomis et al.* [2012]. We performed analysis of variance (ANOVA) tests to identify significant differences in brGDGT distributions between sample types (catchment soil, river, shoreline, Cretaceous, and estuarine)

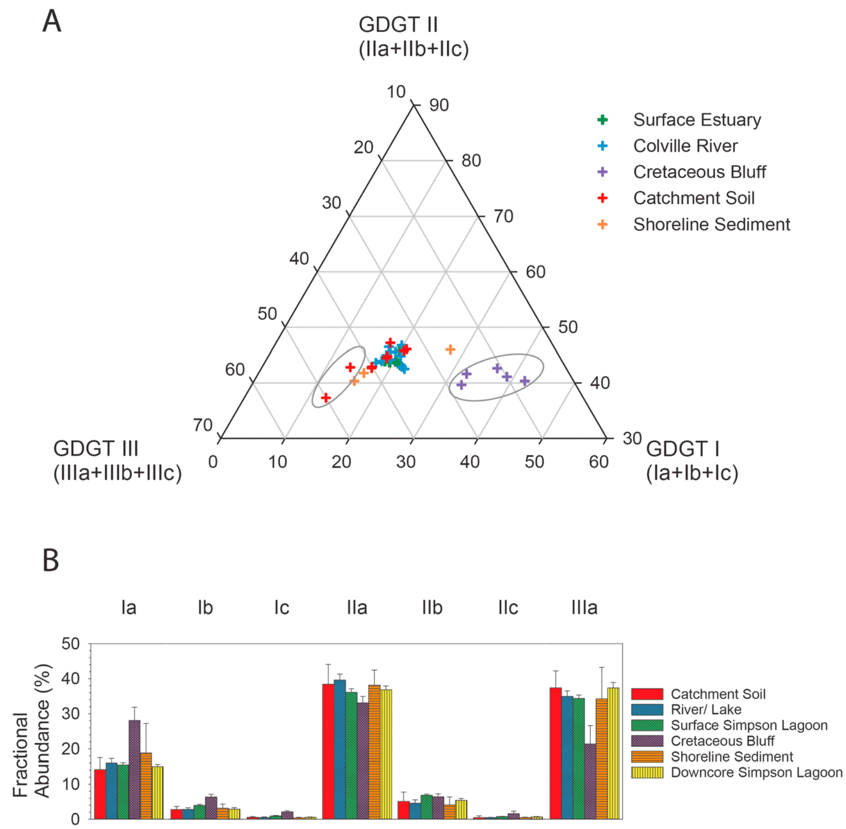

Figure 3. (a) Ternary diagram showing the relationships of the fractional abundances of the tetramethylated, pentamethylated, and hexamethylated branched GDGTs (I, II, and III), including both the 5- and 6-methyl brGDGT isomers. BrGDGT distributions are similar among samples collected from the catchment soil, Colville River, and Simpson Lagoon seabed. Samples collected from Cretaceous outcrops along the Colville River (circled/purple) show significantly higher relative concentrations of GDGT I and lower concentrations of GDGT III compared to the majority of samples. Sediment collected from the Gubik Formation (Pliocene/Pleistocene age, circled/red) have a lower contribution of GDGT I and a higher contribution of GDGT III with respect to other sediment samples. (b) Fractional abundances of the seven brGDGTs utilized in the MBT′ index. The 6-methyl brGDGT isomers were not able to be separately quantified and therefore are included with the respective 5-methyl brGDGT coeluting compounds. Cretaceous age sample brGDGT distributions are significantly different than other samples types. In addition, surface estuarine samples display small, but significant, increases in brGDGTs containing cyclopentane rings with respect to soil, river, and downcore estuarine sediments.

and Holm-Sidak pairwise comparison tests to identify outliers using SigmaPlot 13.0 statistical software. Differences between samples are considered significant if the ANOVA or pairwise comparison test resulted in $p \leq 0.05$ (supporting information Tables S6 and S7).

4. Results

4.1. GDGTs in Surface Sediments From the Colville River, Catchment, and Simpson Lagoon

BrGDGTs in the catchment soil, river, estuarine, and shoreline sediment samples are dominated by the pentamethylated and hexamethylated brGDGTs II (37–47%) and III (26–50%), including both the noncyclopentane-containing (IIa and IIIa) and cyclopentane-containing (IIb, IIc, IIIb, and IIIc) components (Figure 3). The prominence of these particular brGDGTs has been found in other high-latitude soils [*Weijers et al.*, 2007b; *Peterse et al.*, 2009], lakes [*Shanahan et al.*, 2013; *Peterse et al.*, 2014], rivers [*De Jonge et al.*, 2014b; *Peterse et al.*, 2014], and marine environments [*Peterse et al.*, 2009; *Rueda et al.*, 2009] and may reflect an adaptive response to increase membrane fluidity at low temperatures [*Weijers et al.*, 2007b]. While minor variations are evident both within and among sample types; there are no statistically significant differences in the proportions of brGDGTs I, II, and III between any of the surface sediment samples ($p = 0.085$, 0.435, and 0.398, respectively; supporting information Table S6), including the samples collected from the Pliocene/Pleistocene

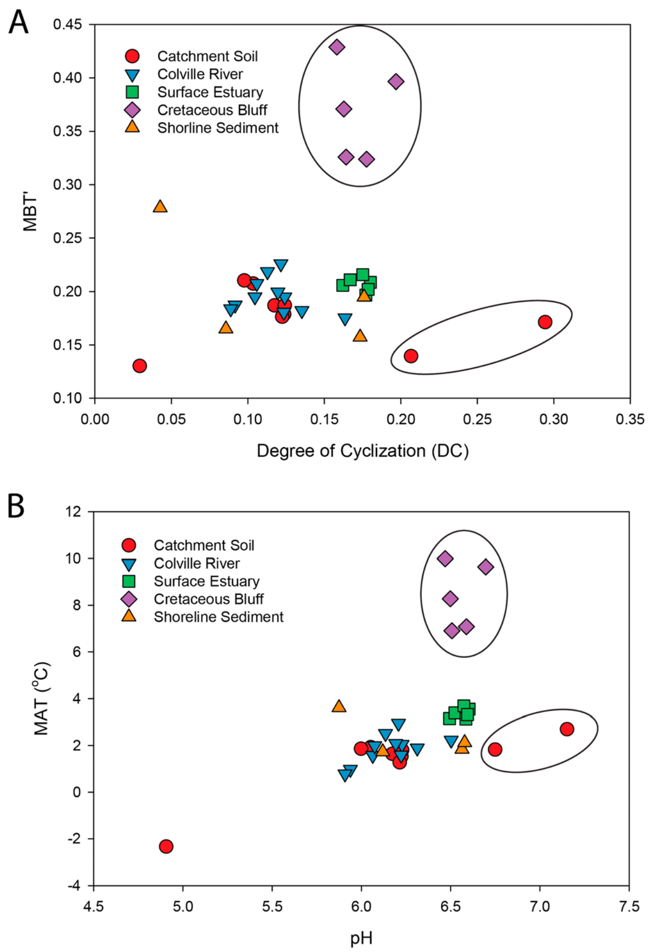

Figure 4. Scatterplots of (a) The methylation index (MBT′) of brGDGT using the modified equation by *Peterse et al.* [2012] versus the degree of cyclization (DC) and (b) reconstructed mean air temperatures (MAT) versus reconstructed soil pH, to enable comparison between different sediment sources in the Colville River study area. Scatterplots reveal good agreement in brGDGT indices and reconstructed temperature and pH among sediments collected from the Colville catchment, river samples, and estuarine (Simpson Lagoon) samples. Sediments collected from older formations (Cretaceous and Pliocene/Pleistocene age) along the Colville River are circled and have values that deviate from the majority of modern soils and fluvial/estuarine sediments.

age Gubik Formation (circled in Figures 3 and 4). In contrast, samples collected from the Cretaceous bluffs located along the west bank of the Colville River do have different brGDGT distributions (GDGTs I and III, $p = < 0.001$), with higher fractional abundances of GDGT I (32–42%) and lower abundances of GDGT III (18–28%) (Figure 3a). In all samples, brGDGTs without cyclopentane moieties (i.e., Ia, IIa, and IIIa) are more abundant than those displaying cyclization (Figure 3b). However, the Cretaceous and surface estuarine sediments do display a slight, but significant increase in the fractional abundance of brGDGTs containing cyclopentane rings with respect to the other sample types ($p = < 0.05$, supporting information Table S7).

Within sample types, the degree of cyclization (DC) is variable, with values ranging from 0.029 to 0.294 (Figure 4a). However, the average values for each sample type (e.g., tundra soil, river sediment, and estuarine sediment) are statistically indistinguishable ($p = 0.085$; supporting information Table S6). Crenarchaeol was detected in all but two of the shoreline samples and two of the samples from the Cretaceous bluffs. However, overall concentrations of the isoprenoid GDGT are low, resulting in a high BIT index for all samples (≥0.87). The majority of soil and river samples have BIT values greater than 0.99 (Figure 5). Simpson Lagoon sediment samples exhibit slightly lower BIT values than riverine samples (0.94–0.96, $p = 0.008$). Computed values of the MBT′ index are also similar for all of the samples except those obtained from the Cretaceous bluffs (Figure 4a and supporting information Table S6).

The pH values calculated from the CBT index are shown in Figures 4b and 5. The catchment soil samples display the largest pH variability, ranging from 4.9 to 7.15. However, differences in the average pH computed for the soil, river/lake, estuarine, shoreline, and Cretaceous sediment samples (6.19 ± 1.22, 6.16 ± 0.34, 6.56 ± 0.08, 6.06 ± 1.288, and 6.55 ± 1.28; errors presented are 2σ) are indistinguishable. With one exception (sample GS15, −2.34 ± 1.0°C), MBT′/CBT reconstructed mean annual temperatures (MAT) for the catchment soil and river sediments fall between 1 and 3 ± 0.7°C using the *Peterse et al.* [2012] global soil calibration (reported uncertainties are based on analytical errors and for purposes of comparison do not include the large calibration uncertainties) (Figure 5). Surface samples from Simpson Lagoon yield MBT′/CBT temperatures (3.13–3.69 ± 0.6°C) that are slightly warmer than those of the river sediment and catchment soils ($p = 0.032$ and 0.004,

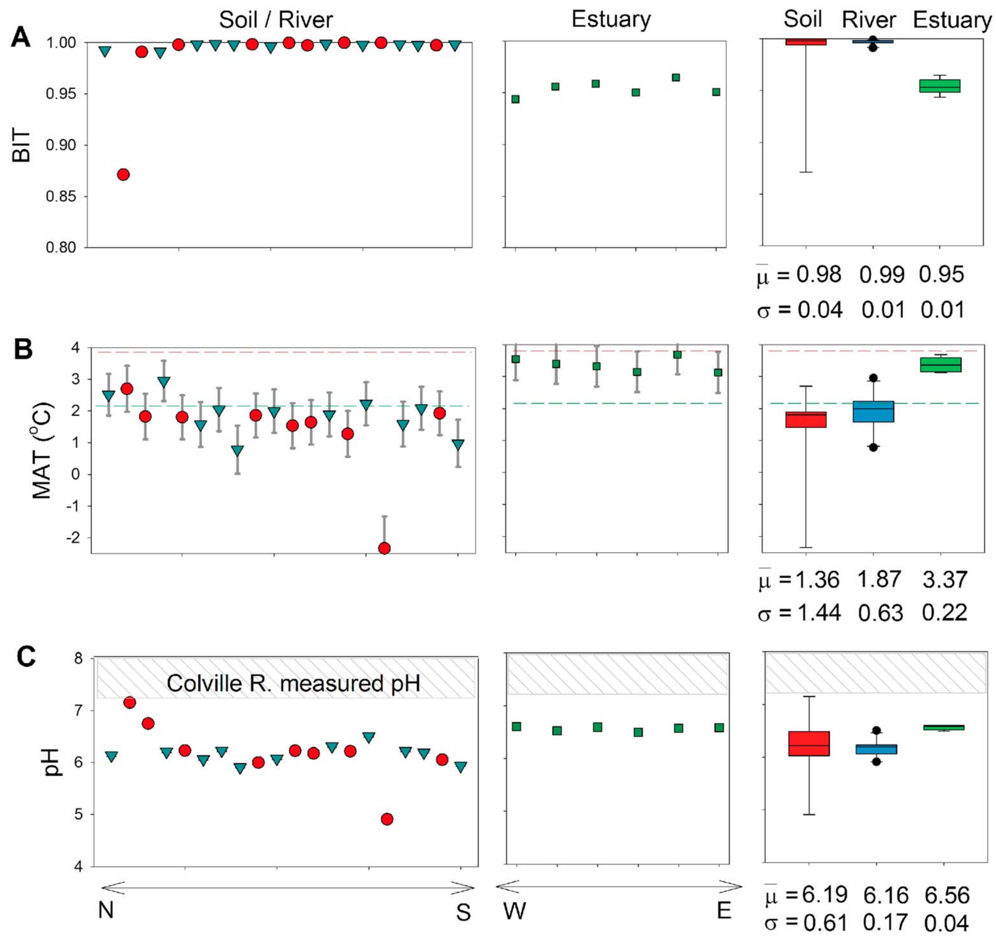

Figure 5. Scatterplots showing variations in (a) BIT index, (b) reconstructed mean air temperature, and (c) reconstructed pH from north to south along the Colville River for soil (red circles) and river sediments (blue triangles) and from west to east in Simpson Lagoon for the estuarine surficial sediments (green squares). Boxplots for each proxy are included for comparison between samples derived from different sources. The red dotted line in Figure 5b is the average measured JJAS temperature from Barrow, AK, in 2010, whereas the green dotted line represents the average instrumental summer (JJAS) temperature over the past 50 years.

respectively; supporting information Table S6). Reconstructed MATs from the Cretaceous bluff sediments are substantially higher, yielding an average temperature of 8.38 ± 2.8°C. As illustrated in Figure 5, there are no apparent spatial trends in BIT, pH, or MAT with distance along the Colville River or with proximity to the delta in Simpson Lagoon.

4.2. Downcore Estuarine Sediment BrGDGTs

BrGDGT distributions for the downcore samples from Simpson Lagoon core SL2 are consistent with those seen in the upstream river and soil samples. BrGDGTs IIa and IIIa are the most abundant, comprising 35–40% and 35–41% of the total, respectively. Crenarchaeol is identifiable in all downcore samples, albeit at relatively low abundances, as indicated by high BIT index values (0.94 to 0.98). Computed MBT′ and CBT indices vary downcore but are consistent with the values obtained for the modern catchment soils and river samples (0.187 ± 0.018 and 0.799 ± 0.102, respectively). The pH values computed from the CBT index do not vary systematically downcore, ranging from 6.1 to 6.6 ($\mu = 6.32 \pm 0.20$) and are consistent with the mean CBT-inferred pH of the river and catchment samples (6.17 ± 0.82). MBT′/CBT-inferred MATs vary between 0.90 and 3.55 ± 0.7°C, with a systematic increase in MAT (~2°C) over the uppermost 35 cm of the core (75 years). The average MAT for this part of the record (2.06 ± 1.04°C) is consistent with the average MAT values computed for the catchment soil and fluvial sediment ($p = 0.52$) (Figure 6).

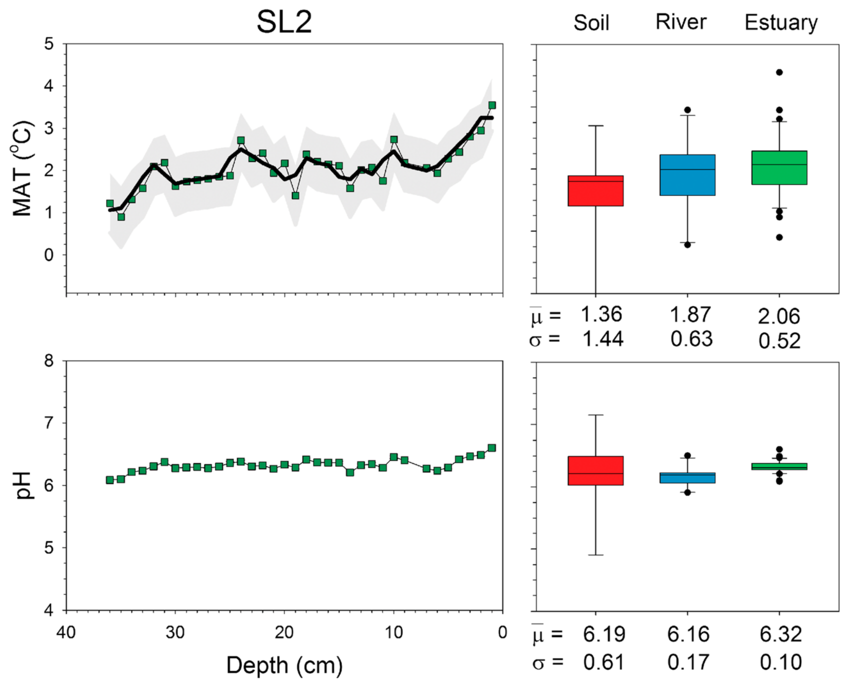

Figure 6. Downcore plots of reconstructed temperature and pH for Simpson Lagoon core SL2 and boxplots comparing average MAT and pH values for estuarine (35 cm average), river, and soil samples. MAT and pH were reconstructed using the *Peterse et al*. [2012] global soil calibration on a 2 year resolution and show little variation in pH and an overall warming trend in MAT. The bold black line included on the temperature reconstruction illustrates the 5 year running average MAT and the grey shading highlights the calculated error in the temperature reconstruction.

5. Discussion

5.1. Sources of BrGDGTs in the Colville River and Simpson Lagoon

Understanding the sources of the brGDGTs preserved in estuarine sediments is crucial to interpreting paleotemperatures reconstructed from fluvially influenced coastal marine sediments. In Simpson Lagoon, brGDGTs may be derived from a combination of catchment soils transported by the Colville River, erosion of shoreline tundra bluffs, fluvial cutbank erosion of Cretaceous sediments (i.e., Prince Creek Fm), aquatic brGDGTs produced in the river and estuary, and in situ brGDGTs produced in marine sediments. Each of these sources may have different brGDGT distributions, resulting either from different environmental conditions at the location of brGDGT production, or from differences in the relationships between brGDGT distributions and environmental conditions in different environmental settings (i.e., aquatic versus terrestrial). If the brGDGTs preserved in the estuarine sediments reflect significant contributions from more than one of these sources, brGDGT temperature reconstructions may not be reliable.

Support for a terrigenous source of the brGDGTs preserved in Simpson Lagoon sediments comes from the high BIT index values (>0.84) observed in the estuarine sediments and the similarity of brGDGT distributions in catchment soil, fluvial, and estuarine samples. Previous studies of brGDGTs in rivers [*Zell et al*., 2013a, 2013b; *De Jonge et al*., 2014b], marine environments [*Zhu et al*., 2011; *Weijers et al*., 2014; *Zell et al*., 2014], and lakes [*Sinninghe Damsté et al*., 2009; *Tierney and Russell*, 2009; *Loomis et al*., 2011] have cited differences in brGDGT distributions between aquatic samples and surrounding soils as evidence for a significant aquatic contribution of brGDGTs. In the Amazon [*Zell et al*., 2013b], Yenisei [*De Jonge et al*., 2014b], and Yangtze Rivers [*Zhu et al*., 2011], suspended particulates showed an increased degree of cyclization compared with watershed soils, resulting in CBT-derived pH values that were elevated relative to catchment soils and more consistent with the measured pH of the river water. Although we were unable to collect suspended particulates from the Colville River during this study, the CBT-derived pH values of the riverbed sediment samples examined here (5.9–6.5) are significantly lower than the measured pH of the Colville River water (7.2–8.0) during the summer months (U.S. Geological Survey). Furthermore, CBT-derived pH values for the fluvial samples are consistent with reported values for the surrounding catchment soils [*Nelson et al*., 1997; *Walker et al*., 1998].

Previous studies of brGDGTs in fluvial and lacustrine environments have shown that MBT/CBT reconstructed temperatures for these systems can differ significantly from those of terrigenous soils, presumably due to in situ aquatic production of brGDGTs [*Tierney and Russell*, 2009; *Tierney et al*., 2010; *Zell et al*., 2013b; *De Jonge et al*., 2014b]. However, MBT′/CBT temperatures for the Colville River sediment samples computed using the soil calibration of *Peterse et al*. [2012] are statistically indistinguishable from the MBT′-/CBT-derived temperatures of the surrounding watershed. In addition, there is no apparent change in brGDGT distributions or calculated brGDGT temperatures (or pH) with distance along the river, as might be expected with increasing aquatic contributions to the brGDGT inventory downstream.

While this data appears to suggest a predominantly soil-derived source of brGDGTs in the Colville River, we cannot rule out the possibility of in situ production occurring within the fluvial system as aquatically produced brGDGTs have displayed similar distributions as the surrounding soil in other Arctic environments. *Peterse et al*. [2014] observed this similarity in brGDGT distributions and resultant pH and temperature reconstructions in two Arctic systems: the Kolyma and Mackenzie Rivers and their corresponding floodplain lakes. Despite the consistency in brGDGT distributions between catchment soils and aqueous environments in these two Arctic systems, concentrations of brGDGTs were found to be higher in the floodplain lakes, suggesting that in situ brGDGT production may still be occurring. *Peterse et al*. [2014] note a global trend in which the distributional offset between brGDGTs produced in aqueous and terrestrial environments decreases with increasing latitude, which they attribute to increasing seasonality and a shorter growing season in Arctic environments. Therefore, even if there is a substantial contribution of aquatically produced brGDGTs within the Colville River, their impact on brGDGT distributions and MBT′-/CBT-derived temperatures are likely to be negligible.

Though the fluvial and catchment soil brGDGT distributions and MBT′/CBT temperatures are indistinguishable, surface sediment samples from the estuary reveal an increased fractional abundance of certain brGDGTs containing cyclopentane rings and yield temperatures that are slightly (but significantly) warmer than those collected from locations upstream and in the catchment soils (Figure 5 and supporting information Tables S6 and S7). The slight differences between the brGDGT distributions in the surface sediments from Simpson Lagoon and the Colville catchment soils may be an indication that there is minor modification from brGDGTs produced in situ within the estuarine setting; however, the same modification in brGDGT distribution is not apparent in the downcore estuarine samples. Increases in the fractional abundance of cyclopentane-containing brGDGTs have been observed in other marine sediments and has been attributed to in situ brGDGT production within a marine water column and/or sediment pore water characterized by higher pH values (Svalbard fjords [*Peterse et al*., 2009], East China Sea [*Zhu et al*., 2011], West African Equatorial Coast [*Weijers et al*., 2014], Amazon Shelf [*Zell et al*., 2014], and Kara Sea [*De Jonge et al*., 2015]). However, sediments in close proximity to river mouths, similar to the Simpson Lagoon/Colville River setting, have exhibited little evidence for modification of brGDGT distributions from marine in situ production [*Zhang et al*., 2012; *Zell et al*., 2014; *De Jonge et al*., 2015].

It is also plausible that the warmer reconstructed temperatures observed in Simpson Lagoon surface sediments, with respect to fluvial/soil samples (1–2°C, Figure 5), result from a contribution of brGDGTs produced within the marine setting, as temperature conditions within the marine environment at the time of in situ brGDGTs production may differ from those of the catchment. In addition, a mixture of modern (aquatically produced) and preaged (soil-derived) brGDGTs within Simpson Lagoon would likely result in warmer reconstructed MATs, as regional temperatures have displayed an overall warming trend over recent decades. However, the variations in temperatures observed between Colville watershed soils and Simpson Lagoon surface sediments are much smaller than seen in other studies [*Zhu et al*., 2011; *Zell et al*., 2014]. For example, *Zell et al*. [2014] found reconstructed temperatures on the Amazon shelf to vary widely and reach as much as 14°C lower than those found in the river, with only the marine sample under the greatest river influence correlating well with fluvial temperatures. In the Yangtze system, *Zhu et al*. [2011] found reconstructed temperatures to be higher on average (up to 10°C difference) in coastal and open shelf environments than in the catchment. Therefore, while there is an indication of in situ brGDGT production within the surface sediments in Simpson Lagoon, the influence of aquatically produced brGDGTs on the MBT′-/CBT-derived temperatures appears to be relatively minor in this Arctic estuarine setting. Thus, it is apparent that the overprinting of in situ brGDGTs in aqueous settings is variable among systems and may be dependent upon the climatic, hydrological, and/or preservational characteristics of the environment.

An alternative explanation is that the estuarine core top samples used here simply reflect a different time interval than the surface grab samples from the river and catchment soils, irrespective of potential in situ aqueous brGDGT production. The surface estuarine samples comprise only the top 1 cm of the Simpson Lagoon sediment cores, while the grab samples collected in the catchment and Colville River have a sediment package thickness of approximately 5–10 cm and therefore likely contain a mixture of older material. Furthermore, the marine core has a higher sedimentation rate (0.46 cm yr^{-1}) than the fluvial cores (~0.1 cm yr^{-1}) and is likely significantly greater than the rate of soil formation. Thus, it is probable that the modern estuary surface samples comprise a shorter time interval (during which temperatures were slightly warmer). The downcore data support this assertion; the mean MBT′/CBT temperature, averaged over the past 75 years, is statistically indistinguishable from the soil and river samples (Figure 6).

Large inputs of eroded, aged material, either from the Cretaceous bluffs exposed along some sections of the Colville River or from the shoreline bluffs bordering the Beaufort Sea, could also alter brGDGT distributions within the Colville River and Simpson Lagoon, respectively. The similarity between the MBT′-/CBT-derived temperatures for the fluvial samples and the surrounding soils suggests that erosion of older Cretaceous sediments are not a major source of brGDGTs in the river and estuary sediments. Cretaceous mean annual temperatures in this part of the Arctic are estimated to have been 6.3–13.3°C [*Spicer and Herman*, 2010]. MBT′/CBT temperatures from Cretaceous sediment samples in the Colville catchment support these estimates, yielding values of 6.9–10°C. The differences in Cretaceous temperatures and brGDGT distributions are large enough to have had an influence on the fluvial and estuarine brGDGT signature, provided the Cretaceous sediments were a significant source of brGDGTs to the fluvial system. The similarities between the modern soil and fluvial MBT′/CBT temperatures indicate that this is unlikely.

The rapid shoreline retreat rates found throughout the Arctic [*Rachold et al*., 2000; *Jones et al*., 2009], indicate that significant contributions of organic material are delivered to marine settings via coastal erosion. This influx of aged, shoreline-derived material could potentially alter brGDGT distributions in Simpson Lagoon; however, we see no evidence for this in our data set. For example, brGDGT-derived MATs calculated for shoreline sediments collected near Oliktok Point, immediately east of the Colville Delta, are statistically indistinguishable from catchment tundra soils. In addition, *Schreiner et al*. [2013] observed increasing contributions of shoreline-derived TOC (total organic carbon) with distance from the Colville Delta (ranging from 15% at SL2 to 85% at SL6); however, temperature reconstructions within Simpson Lagoon do not exhibit significant changes with distance from the river mouth. Furthermore, recent investigations of East Siberian Arctic Shelf sediments and the adjacent terrestrial environments have demonstrated that brGDGT concentrations in the Arctic shoreline bluffs are significantly lower than concentrations present in catchment soils, rivers, and marine sediments [*Peterse et al*., 2014; *Dogrul Selver et al*., 2015; *Sparkes et al*., 2015]. *Sparkes et al*. [2015] found that despite large contributions of organic carbon delivered to the East Siberian Arctic Shelf via coastal erosion (comprising ~50% of marine sediment TOC), nearly 75% of brGDGTs delivered to the shelf were river derived, leading the authors to suggest that brGDGTs may be applicable as a tracer for fluvial TOC in complex Arctic environments. However, marine sediments in the Yenisei Gulf that are removed from the direct influence of the Yenisei River outflow have been found to display brGDGT distributions comparable to the Arctic shoreline sediments [*De Jonge et al*., 2015]. Although brGDGT concentrations were not determined in this study, the lack of evidence for brGDGT distributional offsets in eastern Simpson Lagoon surface samples suggests that shoreline-derived brGDGTs are either a minor contribution or do not significantly impact the estuarine sediment MBT′/CBT temperature estimates.

5.2. BrGDGT-Derived Temperatures Within the Colville Catchment and Simpson Lagoon

5.2.1. Seasonal BrGDGT Production

To assess the accuracy of the brGDGT-derived temperatures within the Colville catchment and Simpson Lagoon and to identify any potential seasonal bias in brGDGT production, we compared the temperature reconstructions with regional instrumental air temperatures from the NOAA National Climatic Data Center. Instrumental temperature records on the North Slope are sparse, with only three temperature records spanning at least two decades. The longest temperature record on the North Slope is from Barrow, AK, located approximately 230 km west of the Colville Delta (1920 through 2010). The record from Barter Island, AK, ~260 km east of the Colville River mouth on the Beaufort Sea Coast, is slightly shorter (1948–1988). Within the Colville catchment, the longest instrumental temperature record is from Umiat, AK (approximately 150 km southwest of the delta), but only covers the interval 1976–2000. Mean annual air temperature (averaged over 1990–2000) for both Umiat, AK, and Barrow, AK is −11°C, significantly lower than the brGDGT-derived average MATs (1.4°C, 1.9°C, 3.4°C, and 2.1°C calculated for soil, river, seabed, and downcore estuarine samples, respectively; Figures 5 and 6).

Whereas the *Peterse et al*. [2012] global soil calibration is a function of mean annual temperature and does not factor in seasonality, the samples from the present study are outside the latitudinal constraints of this soil database. In fact, the MATs for the Colville system sediments are comparable to instrumental summer temperatures (June through September, JJAS), indicating a seasonal influence on brGDGT production. Reconstructed temperatures in the soil and river sediments are approximately 2°C lower than that of the modern summer (2010, JJAS) temperature average from Barrow, AK. They are, however, consistent with the summer temperatures averaged over the past 50 years (Figure 5). In contrast, the Simpson Lagoon surface sediments have reconstructed temperatures only slightly lower than those of modern instrumental averages. The downcore estuarine reconstructed temperatures are also within ± 1°C of the instrumental summer temperature averages from both Barrow, AK, and Barter Island, AK, throughout the majority of the record (Figure 7). While these regional records are not taken directly from our field site, we anticipate comparable temperatures due to the similarity in elevation and location along the Beaufort Sea coast. This is corroborated by *Wendler et al*. [2010], who found that the climate on the coastal plain of the North Slope was fairly uniform based on instrumental observations over the past four decades. Instrumental summer temperatures for Umiat, AK, are on average 3–4°C higher than the reconstructed temperatures for Simpson Lagoon and the recorded JJAS temperatures from coastal Barrow and Barter Island, AK, likely due to its southern inland location. While brGDGT-derived temperatures in marine sediments are assumed to be integrated over the entire catchment, it appears from our data that the majority of brGDGTs in Simpson Lagoon may originate from the arctic coastal plain proximal to the delta.

A seasonal bias in which brGDGT-derived MATs better reflect warm season conditions has previously been suggested for middle- to high-latitude lakes [*Sun et al*., 2011; *Shanahan et al*., 2013; *Loomis et al*., 2014], marine sediments [*Rueda et al*., 2009, 2013; *Moossen et al*., 2015], and soils/peats [*Huguet et al*., 2013; *Pautler et al*., 2014]. In Arctic environments, such as the Colville system, cold temperatures lead to a duration of snow and ice cover from late September through May. During this time, permafrost extends to the soil surface, the river has ice formation up to 2 m thick, and landfast ice covers Simpson Lagoon [*Reimnitz et al*., 1978; *Walker and Hudson*, 2003]. Microbial growth/metabolic activity has been found to decrease at low temperatures such as those found in the Alaskan North Slope permafrost [e.g., *Nedwell*, 1999; *Rivkina et al*., 2000]. In addition, vegetation growth is hindered throughout much of the year due to the cold temperatures, presence of snow and ice, and decreased daylight hours, thus potentially limiting the supply of necessary nutrients to the brGDGT-producing soil bacteria as postulated by *Weijers et al*. [2011]. Therefore, brGDGT temperature reconstructions may be more reflective of the summer months when bacteria are more active. For example, an experimental warming study conducted by *Huguet et al*. [2013] in a French peatland found that brGDGT-derived temperatures over the duration of the experiment exhibited a warming consistent with induced spring/summer temperatures rather than winter temperatures. This seasonal bias may be even more prominent in Arctic environments which are characterized by extreme seasonality [*Pautler et al*., 2014]. It should be noted, however, that the choice of soil calibration has been found to have a significant effect on brGDGT-based temperature reconstructions in Arctic environments, with the original *Weijers et al*. [2007b] equation yielding substantially lower MAT values than the expanded *Peterse et al*. [2012] calibration [*Pautler et al*., 2014; *Peterse et al*., 2014]. This holds true for the Colville system as well, with MATs calculated using the *Weijers et al*. [2007b] calibration that are 5 to 6°C cooler than those derived from the revised MBT′/CBT indices. However, these values are still significantly warmer than the measured mean annual air temperature for the North Slope and lend support to the assertion of seasonal influence.

5.2.2. Downcore Temperature Changes

In addition to the overall agreement with instrumental summer temperatures, the brGDGT-based reconstructed temperatures from the estuarine core reveal an overall trend and magnitude of temperature change over the past 75 years that is significantly correlated with the long instrumental record from Barrow, AK,

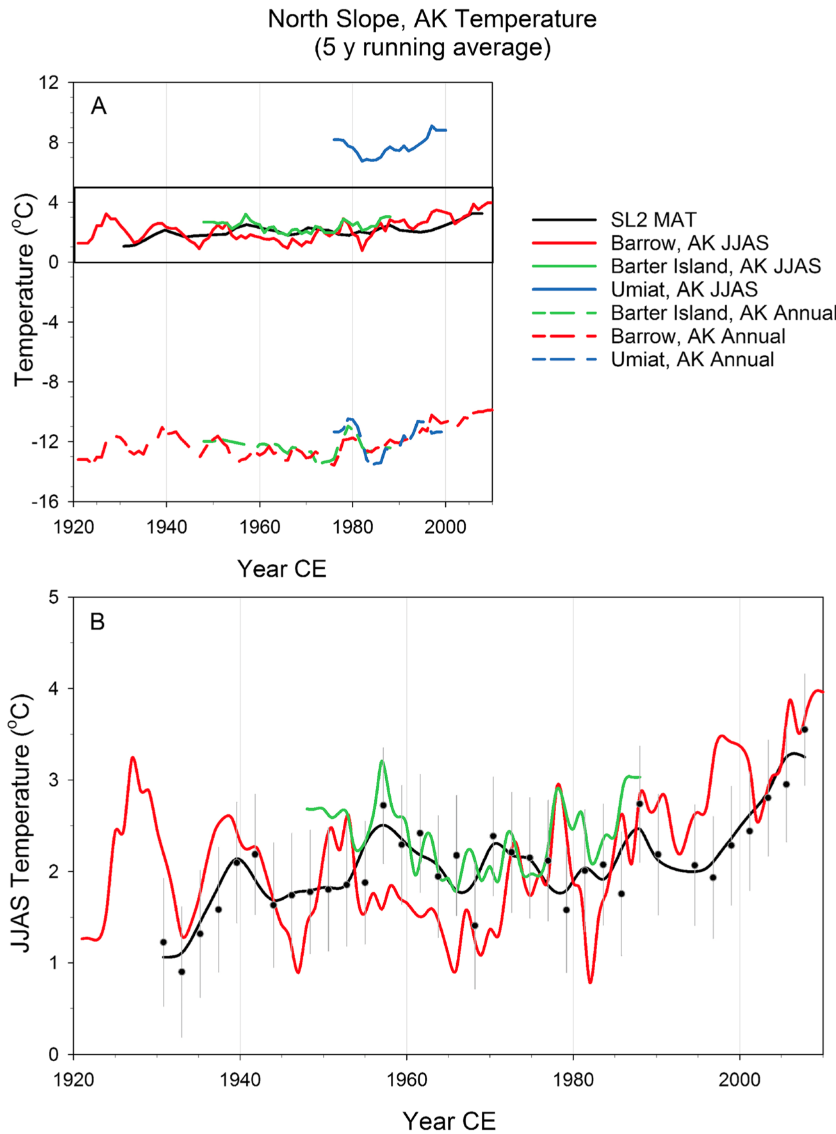

Figure 7. (a) Temperature reconstruction from Simpson Lagoon, AK, using the *Peterse et al.* [2012] calibration compared with average measured annual (dotted) and JJAS (solid) temperatures from Barrow, AK, (red), Barter Island, AK, (green), and Umiat, AK, (blue). (b) Zoomed-in view of comparison between Simpson Lagoon temperature reconstruction (*Peterse et al.* [2012] calibration) and JJAS average temperatures for Barrow, AK, and Barter Island, AK. All temperature records have been smoothed using a 5 year running average. Individual sample data from Simpson Lagoon is presented as discrete points with associated error bars.

($r = 0.45$, $p = 0.008$). Both records reveal an overall warming, consistent with the warming trend observed in other Alaskan locations and throughout the Arctic during the twentieth century [*Serreze et al.*, 2000; *Hinzman et al.*, 2005]. While *Weijers et al.* [2011] suggests a turnover time of approximately 20 years for brGDGTs, our reconstruction indicates that temperature variability can, in fact, be identified on subdecadal timescales. This is consistent with the controlled experiments from *Huguet et al.* [2013] which identified significantly faster turnover time of the brGDGT core lipids in peats (<2 years). Subdecadal-scale resolution in brGDGT-derived temperature records has also been observed in other marine and lake sediment cores [*Rueda et al.*, 2009; *Tyler et al.*, 2010], although this may potentially be related to the incorporation of brGDGTs freshly produced within the aquatic environment. Therefore, we suggest that the MBT′/CBT paleothermometer has the potential to be a useful tool in understanding high-resolution climate variability over the past few millennia assuming brGDGT distributions are accurately reflecting environmental conditions within the catchment.

5.3. Implications for the MBT′/CBT Paleothermometer in Arctic Estuarine Systems

The results of this study indicate that the MBT′/CBT paleothermometer reliably reconstructs temperatures in Simpson Lagoon. Unlike previous studies of larger fluvial systems [*Zhu et al*., 2011; *Zell et al*., 2013a, 2013b; *De Jonge et al*., 2014b], brGDGT distributions in the Colville system are consistent across depositional environments and there is no evidence for significant modification of the brGDGT signal by aquatic production. We hypothesize that this is primarily due to the episodic nature of the Colville River discharge. In addition, the large input of soil-derived brGDGTs to Simpson Lagoon and the high OM preservation potential in Arctic estuaries enables Simpson Lagoon, and potentially other Arctic estuaries, to preserve sedimentary records of brGDGT-derived temperature variations within the catchment.

Studies of fluvial systems have previously suggested that seasonality (e.g., high water season and spring freshet) may affect in situ riverine brGDGT production and, as a result, how closely the fluvial brGDGT distributions reflect the values of the surrounding soils [*Zell et al*., 2013a; *De Jonge et al*., 2015]. For example, brGDGT distributions within the Amazon River were found to be similar to the surrounding soils only during the high water season [*Zell et al*., 2013a]. During this season, the authors found little evidence of in situ production and attribute this to increased runoff during the rainy season. Rivers characterized by episodic sediment transport (e.g., Arctic rivers, small mountainous rivers) deliver the majority of sediment and OM to the coastal ocean during infrequent events, unlike larger rivers, which present little interannual variability in discharge [*Milliman and Syvitski*, 1992; *Wheatcroft et al*., 1997; *Farnsworth and Milliman*, 2003]. Arctic rivers are particularly flood prone due to the rapid breakup of ice and discharge of accumulated snowmelt during a relatively short period of time. In the case of the Colville River, the freshet transports approximately two thirds of the annual sediment load during a few weeks in late spring/early summer [*Walker and Hudson*, 2003; *Rember and Trefry*, 2004]. These episodic rivers may not allow time for the buildup of detectable concentrations of in situ aquatic brGDGTs due to the short residence times of the water. To date, fluvial in situ production has been documented primarily within large river basins, including the Amazon, Yenisei, and Yangtze Rivers [*Zhu et al*., 2011; *Zell et al*., 2013a, 2013b; *De Jonge et al*., 2014b]. Smaller, sediment-laden, episodic rivers, like the Colville, may have a lesser degree of in situ brGDGT production.

Previous research has also illustrated that brGDGT reconstructions in marine sediments require substantial input of terrigenous material as well as high preservation of organic material [*Peterse et al*., 2009; *Zell et al*., 2014]. Since approximately 90–95% of the terrigenously derived material fluvially transported to the Arctic Ocean is trapped in nearshore estuarine environments; Arctic estuarine systems, like Simpson Lagoon, may be well suited for application of the MBT′/CBT temperature proxy [*Gordeev*, 2006]. In recent studies of the Pearl, Yangtze, and Amazon Rivers, BIT values were found to decrease rapidly in estuaries and nearshore environments, often reaching values as low as 0.1 [*Zhu et al*., 2011; *Zhang et al*., 2012; *Zell et al*., 2014]. *Zell et al*. [2014] observed that only the Amazon shelf samples with high BIT values reflected MATs consistent with the Amazon watershed and concluded that settings under high fluvial influence are necessary for brGDGT-based paleoenvironmental reconstructions. While BIT values of sediments from Simpson Lagoon are slightly lower than the fluvial or catchment samples (Figure 5), BIT index values in the lagoon remain above 0.8 for all samples and indicate a dominance of terrigenous material. Similarly, high BIT values have also been observed off the mouths of other Arctic Rivers [*Van Dongen et al*., 2008; *Dogrul Selver et al*., 2012]. In addition, Arctic estuaries have demonstrated a low degree of degradation of organic matter [*Van Dongen et al*., 2008]. This is important, as selective degradation within the marine environment has the potential to alter brGDGT distributions [*Zhu et al*., 2011; *De Jonge et al*., 2015]. *De Jonge et al*. [2015] suggested two potential mechanisms for preferential degradation of brGDGTs in marine environments, the first being that individual brGDGTs may have differing reactivities and thus degrade at different rates. The second, and more likely, mechanism is the preferential degradation of particular brGDGT pools, with brGDGTs produced in situ within aqueous environments being more labile whereas soil-derived brGDGTs may be relatively resistant to degradation, in part due to mineral sorption [*Huguet et al*., 2008; *De Jonge et al*., 2015]. Thus, we suggest that Arctic estuarine environments containing significant soil-derived brGDGTs due to their proximity to sediment-laden, episodic rivers, such as the Colville, may have the highest potential for brGDGT-based temperature reconstructions. However, care should be taken to fully understand the sources of brGDGTs and the potential for modification of brGDGT distributions in river and marine environments before using the MBT′/CBT paleothermometer.

6. Conclusions

This study examines the potential of the MBT′/CBT paleothermometer in an Arctic estuarine environment by investigating the sourcing of brGDGTs in the Colville River and Simpson Lagoon, AK, and comparing reconstructed MATs to regional instrumental temperature records. Recent studies in major river systems and marine environments have identified major modification of brGDGT distributions as a result of in situ production of brGDGTs within the water column, leading to potential complications with the use of this proxy. BrGDGT distributions are consistent throughout the Colville watershed soils, Colville River, and adjacent Simpson Lagoon, suggesting that in situ production within the Colville system has a limited impact on the applicability of the MBT′/CBT paleothermometer.

BrGDGT-derived temperature reconstructions for surficial soil, fluvial, and estuarine samples are in good agreement with regional summer air temperature, displaying mean values between 1.4°C and 3.4°C. The apparent seasonal bias likely results from a limited growing season for soil bacteria in high latitudes which may be due to limited light availability, cold temperatures, and the presence of snow and ice cover throughout the majority of the year. In addition, a high-resolution (2 years) temperature reconstruction over the past ~75 years from Simpson Lagoon reveals an overall twentieth century warming trend consistent with other regional instrumental records along the Beaufort Sea coastline. The prevalence of soil-derived brGDGTs throughout the Colville system in conjunction with the valid temperature reconstructions suggest that Arctic coastal environments adjacent to sediment-laden, episodic rivers may be ideal locations for utilizing the MBT′/CBT paleothermometer; however, consideration of the potential sources of brGDGTs must be taken into account.

In addition, the majority of the published brGDGT temperature records from marine sediments encompass a significantly longer time span with lower resolution [e.g., *Weijers et al*., 2007a; *Bendle et al*., 2010]. The agreement between the Simpson Lagoon brGDGT-derived temperatures and the regional instrumental data suggests that temperatures may be reliably reconstructed on a subdecadal resolution in suitable locations. When extended further in time, high-resolution records, like this Simpson Lagoon record, may be useful for understanding natural climate variability as well as anthropogenic impacts on climate. This is particularly important in regions, such as the Arctic, which are predicted to be most sensitive to future climate change.

Acknowledgments
This research was supported by funding from the National Science Foundation (NSF EAGER grant ARC-0935336 and NSF grant ARC-1203851). A.J.M.H. would also like to acknowledge additional support for the 2012 field program provided by the Alaskan Geological Society. The authors would like to thank Thomas Bianchi for his contributions to the project design and study site selection. We would also like to thank colleagues Kathryn Schreiner, Richard Smith, Mike Rodriguez, and Captain Bill Kopplin of the R/V *Annika Marie* for all of their assistance with the 2010 field work. Assistance during the 2012 field season was provided by Peter Flaig, Dolores van der Kolk, Doug Hissom, and Stephen Hasiotis. We would also like to acknowledge Shannon Loomis for her assistance with the statistical analysis. We also thank the two anonymous reviewers whose comments significantly improved this manuscript. Data for this project can be found in the supporting information.

References

Anderson, V. J., T. M. Shanahan, J. E. Saylor, B. K. Horton, and A. R. Mora (2014), Sources of local and regional variability in the MBT′/CBT paleotemperature proxy: Insights from a modern elevation transect across the Eastern Cordillera of Colombia, *Org. Geochem.*, *69*, 42–51, doi:10.1016/j.orggeochem.2014.01.022.

Arnborg, L., H. J. Walker, and J. Peippo (1967), Suspended load in the Colville River, Alaska, 1962, *Geogr. Ann.*, *49A*, 131–144.

Bendle, J. A., J. W. H. Weijers, M. A. Maslin, J. S. Sinninghe Damsté, S. Schouten, E. C. Hopmans, C. S. Boot, and R. D. Pancost (2010), Major changes in glacial and Holocene terrestrial temperatures and sources of organic carbon recorded in the Amazon fan by tetraether lipids, *Geochem. Geophys. Geosyst.*, *11*, Q12007, doi:10.1029/2010GC003308.

Besonen, M. R., W. Patridge, R. S. Bradley, P. Francus, J. S. Stoner, and M. B. Abbott (2008), A record of climate over the last millennium based on varved lake sediments from the Canadian High Arctic, *Holocene*, *18*(1), 169–180.

Bianchi, T. S., and M. A. Allison (2009), Large-river delta-front estuaries as natural "recorders" of global environmental change, *Proc. Natl. Acad. Sci. U.S.A.*, *106*(20), 8085–8092, doi:10.1073/pnas.0812878106.

Blaga, C. I., G. J. Reichart, O. Heiri, and J. S. Sinninghe Damsté (2009), Tetraether membrane lipid distributions in water-column particulate matter and sediments: A study of 47 European lakes along a north-south transect, *J. Paleolimnol.*, *41*, 523–540.

Bradley, R. S. (1990), Holocene paleoclimatology of the Queen Elizabeth Islands, Canadian High Arctic, *Quat. Sci. Rev.*, *9*, 365–384.

Craig, P. C., and P. J. McCart (1975), Classification of stream types in Beaufort Sea drainages between Prudhoe Bay, Alaska, and the MacKenzie Delta, N.W.T., Canada, *Arct. Alp. Res.*, *7*(2), 183–198.

De Jonge, C., E. C. Hopmans, A. Stadnitskaia, W. I. C. Rijpstra, R. Hofland, E. Tegelaar, and J. S. Sinninghe Damsté (2013), Identification of novel penta- and hexamethylated branched glycerol dialkyl glycerol tetraethers in peat using HPLC-MS^2, GC-MS and GC-SMB-MS, *Org. Geochem.*, *54*, 78–82, doi:10.1016/j.orggeochem.2012.10.004.

De Jonge, C., E. C. Hopmans, C. I. Zell, J. H. Kim, S. Schouten, and J. S. Sinninghe Damsté (2014a), Occurrence and abundance of 6-methyl branched glycerol dialkyl glycerol tetraethers in soils: Implications for palaeoclimate reconstruction, *Geochim. Cosmochim. Acta*, *141*, 97–112, doi:10.1016/j.gca.2014.06.013.

De Jonge, C., A. Stadnitskaia, E. C. Hopmans, G. Cherkashov, A. Fedotov, and J. S. Sinninghe Damsté (2014b), In situ produced branched glycerol dialkyl glycerol tetraethers in suspended particulate matter from the Yenisei River, Eastern Siberia, *Geochim. Cosmochim. Acta*, *125*, 476–491, doi:10.1016/j.gca.2013.10.031.

De Jonge, C., A. Stadnistskaia, E. C. Hopmans, G. Cherkashov, A. Fedotov, I. D. Streletskaya, A. A. Vasiliev, and J. S. Sinninghe Damsté (2015), Drastic changes in the distribution of branched tetraether lipids in suspended matter and sediments from the Yenisei River and Kara Sea (Siberia): Implications for the use of brGDGT-based proxies in coastal marine sediments, *Geochim. Cosmochim. Acta*, *165*, 200–225, doi:10.1016/j.gca.2015.05.044.

De Jonge, C., A. Stadnitskaia, G. Cherkashov, and J. S. Sinninghe Damsté (2016), Branched glycerol dialkyl glycerol tetraethers and crenarchaeol record post-glacial sea level rise and shift in source of terrigenous brGDGTs in the Kara Sea (Arctic Ocean), *Org. Geochem.*, *92*, 42–54, doi:10.1016/j.orggeochem.2015.11.009.

Ding, S., Y. Xu, Y. Wang, Y. He, J. Hou, L. Chen, and J. S. He (2015), Distributions of glycerol dialkyl glycerol tetraethers in surface soils of Quinghai-Tibetan Plateau: Implications of GDGT-based proxies in cold and dry regions, *Biogeosci. Discuss.*, *12*, 481–513, doi:10.5194/bgd-12-481-2015.

Dogrul Selver, A., H. M. Talbot, O. Gustafsson, S. Boult, and B. E. van Dongen (2012), Soil organic matter transport along an sub-Arctic river-sea transect, *Org. Geochem.*, *51*, 63–72, doi:10.1016/j.orggeochem.2012.08.002.

Dogrul Selver, A., R. B. Sparkes, J. Bischoff, H. M. Talbot, O. Gustafsson, I. P. Semiletov, O. V. Dudarev, S. Boult, and B. E. van Dongen (2015), Distributions of bacterial and archaeal membrane lipids in surface sediments reflect differences in input and loss of terrestrial organic carbon along a cross-shelf Arctic transect, *Org. Geochem.*, *83–84*, 16–26, doi:10.1016/j.orggeochem.2015.01.005.

Efron, B. (1979), Bootstrap methods: Another look at the Jackknife, *Ann. Stat.*, *7*(1), 1–26.

Eisner, W. R., J. G. Bockheim, K. M. Hinkel, T. A. Brown, F. E. Nelson, K. M. Peterson, and B. M. Jones (2005), Paleoenvironmental analyses of an organic deposit from an erosional landscape remnant, Arctic Coastal Plain of Alaska, *Palaeogeogr. Palaeoclimatol. Palaeoecol.*, *217*, 187–204.

Evison, L. H., P. E. Calkin, and J. M. Ellis (1996), Late-Holocene glaciation and twentieth-century retreat, northeastern Brooks Range, Alaska, *Holocene*, *6*(1), 17–24.

Farnsworth, K. L., and J. D. Milliman (2003), Effects of climatic and anthropogenic change on small mountainous rivers: The Salinas River example, *Global Planet. Change*, *39*, 53–64, doi:10.1016/S0921-8181(03)00017-1.

Flaig, P. P., P. J. McCarthy, and A. R. Fiorillo (2011), A tidally-influenced, high latitude coastal-plain: The Upper Cretaceous (Maastrichtian) Prince Creek Formation, North Slope, Alaska, in *From River to Rock Record: The Preservation of Fluvial Sediments and Their Subsequent Interpretation: Society for Sedimentary Geology*, *Spec. Publ*., vol. 97, edited by S. K. Davidson et al., pp. 233–264, SEPM, Tulsa, Okla.

Gordeev, V. V. (2006), Fluvial sediment flux to the Arctic Ocean, *Geomorphology*, *80*, 94–104, doi:10.1016/j.geomorph.2005.09.008.

Gordeev, V. V., J. M. Martin, I. S. Sidorov, and M. V. Sidorova (1996), A reassessment of the Eurasian river input of water, sediment, major elements, and nutrients to the Arctic Ocean, *Am. J. Sci.*, *296*, 664–691.

Hanna, A. J. M., M. A. Allison, T. S. Bianchi, F. Marcantonio, and J. A. Goff (2014), Late Holocene sedimentation in a high Arctic coastal setting: Simpson Lagoon and Colville Delta, Alaska, *Cont. Shelf Res.*, *74*, 11–24.

Hinzman, L. D., et al. (2005), Evidence and implications of recent climate change in Northern Alaska and other Arctic regions, *Clim. Change*, *72*, 251–298, doi:10.1007/s10584-005-5352-2.

Holland, M. M., and C. M. Bitz (2003), Polar amplification of climate change in coupled models, *Clim. Dyn.*, *21*(3–4), 221–232.

Hopmans, E. C., J. W. H. Weijers, E. Schefub, L. Herfort, J. S. Sinninghe Damsté, and S. Schouten (2004), A novel proxy for terrestrial organic matter in sediments based on branched and isoprenoid tetraether lipids, *Earth Planet. Sci. Lett.*, *224*, 107–116.

Huguet, A., C. Fosse, F. Laggoun-Defarge, F. Delarue, and S. Derenne (2013), Effects of a short-term experimental microclimate warming on the abundance and distribution of branched GDGTs in a French peatland, *Geochim. Cosmochim. Acta*, *105*, 294–315, doi:10.1016/j.gca.2012.11.037.

Huguet, C., G. J. de Lange, O. Gustafsson, J. J. Middelburg, J. S. Sinninghe Damsté, and S. Schouten (2008), Selective preservation of soil organic matter in oxidized marine sediments (Madeira Abyssal Plain), *Geochim. Cosmochim. Acta*, *72*(24), 6061–6068, doi:10.1016/j.gca.2008.09.021.

Intergovernmental Panel on Climate Change (2013), *Climate Change 2013: The Physical Science Basis. Contribution of Working Group I to the Fifth Assessment Report of the Intergovernmental Panel on Climate Change*, edited by T. F. Stocker et al., pp. 1535, Cambridge Univ. Press, Cambridge, U. K., and New York.

Jones, B. M., C. D. Arp, M. T. Jorgenson, K. M. Hinkel, J. A. Schmutz, and P. L. Flint (2009), Increase in the rate and uniformity of coastline erosion in Arctic Alaska, *Geophys. Res. Lett.*, *36*, L03503, doi:10.1029/2008GL036205.

Jorgenson, M. T., and J. Brown (2005), Classification of the Alaskan Beaufort Sea Coast and estimation of carbon and sediment inputs from coastal erosion, *Geo Mar. Lett.*, *25*, 69–80.

Jorgenson, M. T., Y. L. Shur, and E. R. Pullman (2006), Abrupt increase in permafrost degradation in Arctic Alaska, *Geophys. Res. Lett.*, *33*, L02503, doi:10.1029/2005GL024960.

Lachenbruch, A. H., and B. V. Marshall (1969), Heat flow in the Arctic, Arctic, 22 (3), Proceedings of the U.S. Naval Arctic Research Laboratory, 300-311.

Loomis, S. E., J. M. Russell, and J. S. Sinninghe Damsté (2011), Distributions of branched GDGTs in soils and lake sediments from western Uganda: Implications for a lacustrine paleothermometer, *Org. Geochem.*, *42*, 739–751, doi:10.1016/j.orggeochem.2011.06.004.

Loomis, S. E., J. M. Russell, B. Ladd, F. A. Street-Perrott, and J. S. Sinninghe Damsté (2012), Calibration and application of the branched GDGT temperature proxy on East African lake sediments, *Earth Planet. Sci. Lett.*, *357–358*, 277–288, doi:10.1016/j.epsl.2012.09.031.

Loomis, S. E., J. M. Russell, A. M. Heureux, W. J. D'Andrea, and J. S. Sinninghe Damsté (2014), Seasonal variability of branched glycerol dialkyl glycerol tetraethers (brGDGTs) in a temperate lake system, *Geochim. Cosmochim. Acta*, *144*, 173–187, doi:10.1016/j.gca.2014.08.027.

Mahoney, A., H. Eicken, A. G. Gaylord, and L. Shapiro (2007), Alaska landfast sea ice: Links with bathymetry and atmospheric circulation, *J. Geophys. Res.*, *112*, C02001, doi:10.1029/2006JC003559.

Mars, J. C., and D. W. Houseknecht (2007), Quantitative remote sensing study indicates doubling of coastal erosion rate in past 50 yr along a segment of the Arctic coast of Alaska, *Geology*, *35*(7), 583–586, doi:10.1130/G23672A.1.

McKay, N. P., and D. S. Kaufman (2014), An extended Arctic proxy temperature database for the past 2,000 years, *Sci. Data*, *1*, 140026, doi:10.1038/sdata.2014.26.

Milliman, J. D., and J. P. M. Syvitski (1992), Geomorphic/tectonic control of sediment discharge to the ocean: The importance of small mountainous rivers, *J. Geol.*, *100*(5), 525–544.

Moore, T. E., W. K. Wallace, K. J. Bird, S. M. Karl, C. G. Mull, and J. T. Dillon (1994), Geology of northern Alaska, in *The Geology of Alaska*, *Geol. North America*, vol. G-1, edited by G. Plafker and H. C. Berg, pp. 49–140, Geol. Soc. of Am., Boulder, Colo.

Moossen, H., J. Bendle, O. Seki, U. Quillmann, and K. Kawamura (2015), North Atlantic Holocene climate evolution recorded by high-resolution terrestrial and marine biomarker records, *Quat. Sci. Rev.*, *129*, 111–127, doi:10.1016/j.quascirev.2015.10.013.

Nedwell, D. B. (1999), Effect of low temperature on microbial growth: Lowered affinity for substrates limits growth at low temperature, *Microb. Ecol.*, *30*(2), 101–111, doi:10.1111/j.1574-6941.1999.tb00639.x.

Nelson, F. E., N. I. Shiklomanov, G. R. Mueller, K. M. Hinkel, D. A. Walker, and J. G. Bockheim (1997), Estimating Active-layer thickness over a large region: Kuparuk River Basin, Alaska, USA, *Arct. Alp. Res.*, *29*(4), 367–378.

Osterkamp, T. E., and M. W. Payne (1981), Estimates of permafrost thickness from well logs in northern Alaska, *Cold Reg. Sci. Technol.*, *5*, 13–27.

Overpeck, J., et al. (1997), Arctic environmental change of the last four centuries, *Science*, *278*, 1251–1256, doi:10.1126/science.278.5341.1251.

Pautler, B. G., G. J. Reichart, P. T. Sanborn, M. J. Simpson, and J. W. H. Weijers (2014), Comparison of soil derived tetraether membrane lipid distributions and plant-wax δD compositions for reconstruction of Canadian Arctic temperatures, *Palaeogeogr. Palaeoclimatol. Palaeoecol.*, *404*, 78–88, doi:10.1016/j.palaeo.2014.03.038.

Pearson, E. J., S. Juggins, H. M. Talbot, J. Weckstrom, P. Rosen, D. B. Ryves, S. J. Roberts, and R. Schmidt (2011), A lacustrine GDGT-temperature calibration from the Scandinavian Arctic to Antarctic: Renewed potential for the application of GDGT-paleothermometry in lakes, *Geochim. Cosmochim. Acta*, *75*, 6225–6238, doi:10.1016/j.gca.2011.07.042.

Peterse, F., J. H. Kim, S. Schouten, D. K. Kristensen, N. Koc, and J. S. Sinninghe Damsté (2009), Constraints on the application of the MBT/CBT palaeothermometer at high latitude environments (Svalbard, Norway), *Org. Geochem.*, *40*, 692–699, doi:10.1016/j.orggeochem.2009.03.004.

Peterse, F., J. van der Meer, S. Schouten, J. W. H. Weijers, N. Fierer, R. B. Jackson, J. H. Kim, and J. S. Sinninghe Damsté (2012), Revised calibration of the MBT-CBT paleotemperature proxy based on branched tetraether membrane lipids in surface soils, *Geochim. Cosmochim. Acta*, *96*, 215–229, doi:10.1016/j.gca.2012.08.011.

Peterse, F., J. E. Vonk, R. M. Holmes, L. Giosan, N. Zimov, and T. Eglinton (2014), Branched glycerol dialkyl glycerol tetraethers in Arctic lake sediments: Sources and implications for paleothermometry at high latitudes, *J. Geophys. Res. Biogeosci.*, *119*, 1738–1754, doi:10.1002/2014JG002639.

Rachold, V., M. N. Grigoriev, F. E. Are, S. Solomon, E. Reimnitz, H. Kassens, and M. Antonow (2000), Coastal erosion vs riverine sediment discharge in the Arctic Shelf seas, *Int. J. Earth Sci.*, *89*, 450–460, doi:10.1007/s005310000113.

Reimnitz, E., L. Toimil, and P. Barnes (1978), Arctic continental shelf morphology related to sea-ice zonation, Beaufort Sea, Alaska, *Mar. Geol.*, *28*, 179–210.

Rember, R. D., and J. H. Trefry (2004), Increased concentrations of dissolved trace metals and organic carbon during snowmelt in rivers of the Alaskan Arctic, *Geochim. Cosmochim. Acta*, *68*, 477–489.

Rivkina, E. M., E. I. Friedmann, C. P. McKay, and D. A. Gilichinsky (2000), Metabolic activity of permafrost bacteria below the freezing point, *Appl. Environ. Microbiol.*, *66*(8), 3230–3233, doi:10.1128/AEM.66.8.3230-3233.2000.

Rueda, G., A. Rosell-Mele, M. Escala, R. Gyllencreutz, and J. Backman (2009), Comparison of instrumental and GDGT-based estimates of sea surface and air temperatures from the Skagerrak, *Org. Geochem.*, *40*, 287–291, doi:10.1016/j.orggeochem.2008.10.012.

Rueda, G., S. Fietz, and A. Rosell-Mele (2013), Coupling of air and sea surface temperatures in the eastern Fram Strait during the last 2000 years, *Holocene*, *23*(5), 692–698, doi:10.1177/0959683612470177.

Schouten, S., C. Huguet, E. C. Hopmans, M. V. M. Kienhuis, and J. S. Sinninghe Damsté (2007), Analytical methodology for TEX_{86} paleothermometry by high-performance liquid chromatography/atmospheric pressure chemical ionization-mass spectrometry, *Anal. Chem.*, *79*, 2940–2944.

Schreiner, K. M., T. S. Bianchi, T. I. Eglinton, M. A. Allison, and A. J. M. Hanna (2013), Sources of terrigenous inputs to surface sediments of the Colville River Delta and Simpson's Lagoon, Beaufort Sea, Alaska, *J. Geophys. Res. Biogeosci.*, *118*, 808–824, doi:10.1002/jgrg.20065.

Schuur, E. A. G., et al. (2015), Climate change and the permafrost carbon feedback, *Nature*, *520*, 171–179, doi:10.1038/nature14338.

Serreze, M. C., and R. G. Barry (2011), Processes and impacts of arctic amplification: A research synthesis, *Global Planet. Change*, *77*(1–2), 85–96, doi:10.1016/j.gloplacha.2011.03.004.

Serreze, M. C., J. E. Walsh, F. S. Chapin III, T. Osterkamp, M. Dyurgerov, V. Romanovsky, W. C. Oechel, J. Morison, T. Zhang, and R. G. Barry (2000), Observational evidence of recent change in the northern high-latitude environment, *Clim. Change*, *46*, 159–207.

Shanahan, T. M., K. A. Hughen, and B. A. S. Van Mooy (2013), Temperature sensitivity of branched and isoprenoid GDGTs in Arctic lakes, *Org. Geochem.*, *64*, 119–128, doi:10.1016/j.orggeochem.2013.09.010.

Sinninghe Damsté, J. S., E. C. Hopmans, R. D. Pancost, S. Schouten, and J. A. J. Geenevasen (2000), Newly discovered non-isoprenoid glycerol dialkyl glycerol tetraether lipids in sediments, *Chem. Commun.*, *17*, 1683–1684, doi:10.1039/B0045171.

Sinninghe Damsté, J. S., J. Ossebaar, B. Abbas, S. Schouten, and D. Verschuren (2009), Fluxes and distribution of tetraether lipids in an equatorial African lake: Constraints on the application of the TEX86 palaeothermometer and BIT index in lacustrine settings, *Geochim. Cosmochim. Acta*, *73*(14), 4232–4249, doi:10.1016/j.gca.2009.04.022.

Sparkes, R. B., A. Dogrul Selver, J. Bischoff, H. M. Talbot, O. Gustafsson, I. P. Semiletov, O. V. Dudarev, and B. E. van Dongen (2015), GDGT distributions on the East Siberian Arctic Shelf: Implications for organic carbon export, burial and degradation, *Biogeosciences*, *12*, 3753–3768, doi:10.5194/bg-12-3753-2015.

Spicer, R. A., and A. B. Herman (2010), The Late Cretaceous environment of the Arctic: A quantitative reassessment based on plant fossils, *Palaeogeogr. Palaeoclimatol. Palaeoecol.*, *295*(3–4), 423–442, doi:10.1016/j.palaeo.2010.02.025.

Stone, R. S., D. Longenecker, E. G. Dutton, and J. M. Harris (2001), The advancing date of Spring snowmelt in the Alaskan Arctic, Eleventh ARM Science Team Meeting Proceedings, Atlanta, Georgia, March 19–23, 2001.

Sun, Q., G. Chu, M. Liu, M. Xie, S. Li, Y. Ling, X. Wang, L. Shi, G. Jia, and H. Lue (2011), Distributions and temperature dependence of branched glycerol dialkyl glycerol tetraethers in recent lacustrine sediments from China and Nepal, *J. Geophys. Res.*, *116*, G01008, doi:10.1029/2010JG001365.

Tierney, J. E., and J. M. Russell (2009), Distributions of branched GDGTs in a tropical lake system: Implications for lacustrine application of the MBT/CBT paleoproxy, *Org. Geochem.*, *40*, 1032–1036.

Tierney, J. E., J. M. Russell, H. Eggermont, E. C. Hopmans, D. Verschuren, and J. S. Sinninghe Damsté (2010), Environmental controls on branched tetraether lipid distributions in tropical East African lake sediments, *Geochim. Cosmochim. Acta*, *74*, 4902–4918, doi:10.1016/j.gca.2010.06.002.

Tyler, J. J., A. J. Nederbragt, V. J. Jones, and J. W. Thurow (2010), Assessing past temperature and soil pH estimates from bacterial tetraether membrane lipids: Evidence from the recent lake sediments of Lochnagar, Scotland, *J. Geophys. Res.*, *115*, G01015, doi:10.1029/2009JG001109.

Van Dongen, B. E., I. Semiletov, J. W. H. Weijers, and O. Gustafsson (2008), Contrasting lipid biomarker composition of terrestrial organic matter exported from across the Eurasian Arctic by the five great Russian Arctic rivers, *Global Biogeochem. Cycles*, *22*, GB1011, doi:10.1029/2007GB002974.

Walker, D. A., et al. (1998), Energy and trace-gas fluxes across a soil pH boundary in the Arctic, *Nature*, *394*, 469–472.

Walker, H. J. (1975), Intermittent streams and their influence on landforms, *Catena*, *2*, 181–192.

Walker, H. J. (1998), Arctic deltas, *J. Coastal Res.*, *14*, 718–738.

Walker, H. J., and P. F. Hudson (2003), Hydrologic and geomorphic processes in the Colville River Delta, Alaska, *Geomorphology*, *56*, 291–303.

Weijers, J. W. H., S. Schouten, E. C. Hopmans, J. A. J. Geenevasen, O. R. P. David, J. M. Coleman, R. D. Pancost, and J. S. Sinninghe Damsté (2006), Membrane lipids of mesophilic anaerobic bacteria thriving in peats have typical archaeal traits, *Environ. Microbiol.*, *8*(4), 648–657, doi:10.1111/j.1462-2920.2005.D0941.

Weijers, J. W. H., E. Schefub, S. Schouten, and J. S. Sinninghe Damsté (2007a), Coupled thermal and hydrological evolution of tropical Africa over the last deglaciation, *Science*, *315*(5819), 1701–1704, doi:10.1126/science.1138131.
Weijers, J. W. H., S. Schouten, J. C. van den Donker, E. C. Hopmans, and J. S. Sinninghe Damsté (2007b), Environmental controls on bacterial tetraether membrane lipid distribution in soils, *Geochim. Cosmochim. Acta*, *71*, 703–713, doi:10.1016/j.gca.2006.10.003.
Weijers, J. W. H., B. Bernhardt, F. Peterse, J. P. Werne, J. A. J. Dugnait, S. Schouten, and J. S. Sinninghe Damsté (2011), Absence of seasonal patterns in MBT-CBT indices in mid-latitude soils, *Geochim. Cosmochim. Acta*, *75*(11), 3179–3190, doi:10.1016/j.gca.2011.03.015.
Weijers, J. W. H., E. Schefub, J. H. Kim, J. S. Sinninghe Damsté, and S. Schouten (2014), Constraints on the sources of branched tetraether membrane lipids in distal marine sediments, *Org. Geochem.*, *72*, 14–22, doi:10.1016/j.orggeochem.2014.04.011.
Wendler, G., M. Shulski, and B. Moore (2010), Changes in the climate of the Alaskan North Slope and the ice concentration of the adjacent Beaufort Sea, *Theor. Appl. Climatol.*, *99*, 67–74, doi:10.1007/s00704-009-0127-8.
Wheatcroft, R. A., C. K. Sommerfield, D. E. Drake, J. C. Borgeld, and C. A. Nittrouer (1997), Rapid and widespread dispersal of flood sediment on the northern California margin, *Geology*, *25*(2), 163–166.
Zell, C., J. H. Kim, G. Abril, R. L. Sobrinho, D. Dorhout, P. Moreira-Turcq, and J. S. Sinninghe Damsté (2013a), Impact of seasonal hydrological variation on the distributions of tetraether lipids along the Amazon River in the central Amazon basin: Implications for the MBT/CBT paleothermometer and the BIT index, *Front. Microbiol.*, *4*, 228, doi:10.3389/fmicb.2013.00228.
Zell, C., J. H. Kim, P. Moreira-Turcq, G. Abril, E. C. Hopmans, M. P. Bonnet, R. L. Sobrinho, and J. S. Sinninghe Damsté (2013b), Disentangling the origins of branched tetraether lipids and crenarchaeol in the lower Amazon River: Implications for GDGT-based proxies, *Limnol. Oceanogr.*, *58*(1), 343–353, doi:10.4319/lo.2013.58.1.0343.
Zell, C., J. H. Kim, D. Hollander, L. Lorenzoni, P. Baker, C. G. Silva, C. Nittrouer, and J. S. Sinninghe Damsté (2014), Sources and distributions of branched and isoprenoid tetraether lipids on the Amazon shelf and fan: Implications for the use of GDGT-based proxies in marine sediments, *Geochim. Cosmochim. Acta*, *139*, 293–312, doi:10.1016/j.gca.2014.04.038.
Zhang, C. L., J. Wang, Y. Wei, C. Zhu, L. Huang, and H. Dong (2012), Production of branched tetraether lipids in the lower Pearl River and estuary: Effects of extraction methods and impact on bGDGT proxies, *Front. Microbiol.*, *2*, 274, doi:10.3389/fmicb.211.00274.
Zhu, C., J. W. H. Weijers, T. Wagner, J. M. Pan, J. F. Chen, and R. D. Pancost (2011), Sources and distributions of tetraether lipids in surface sediments across a large river-dominated continental margin, *Org. Geochem.*, *42*, 376–386, doi:10.1016/j.orggeochem.2011.02.002.